5

Smart Hydrogel for Stiffness Controllable Continuum Manipulators: A Conceptual Design

Daniel Guevara Mosquera[1], S.M. Hadi Sadati[1,3], Kaspar Althoefer[2] and Thrishantha Nanayakkara[3]

[1]Center for Robotic Research (CoRe), King's College London, London, United Kingdom
[2]School of Engineering and Materials Science, Queen Mary University of London, London, United Kingdom
[3]Dyson School of Design Engineering, Imperial College London, London, United Kingdom

Abstract

As it was discussed in previous chapters of Part I, soft continuum trunk and tentacle manipulators have high inherent dexterity and reconfigurability and have become an attractive candidate for safe manipulation and explorations in surgical and space robotic applications, recently. However, achieving accuracy in precise tasks is a challenge with these highly flexible structures, for which stiffness variable designs based on jamming, smart material, antagonistic actuation, and morphing structures have been introduced in the recent years. In this chapter, variable stiffness properties of an electroactive poly (sodium acrylate) (pNaAc) hydrogel are tested. An anisotropic stiffness ion pattern is printed on the hydrogel straps giving them shape memory properties. The hydrogel swells up to two times its original size and soften (4.2-0 KN/m) in an ethanol aquatic solution depending on the ethanol saturation while preserving its programmed shape. Changing the solution ethanol saturation can be used to control the hydrogel stiffness based of which a conceptual design for a stiffness controllable STIFF-FLOP module is presented and will be fabricated in the future.

5.1 Introduction

Performing complicated biological tasks such as manipulation in unpredictable conditions where safe interaction with the environment is important requires dexterity and compliance in which low actuation energy, high dexterity, reachability, maneuverability, back drivability, and self adjustablbility of continuum mechanisms are shown to be advantageous [1]. In nature, biological creatures benefit from compliant muscle-tendon-bone structures capable of exerting instantaneous high-peak forces and velocities necessary for such tasks [2]. On the other hand, to address the common problems with current actuation methods in robotics research, such as back-drivability, stiffness control, and energy consumption, different methods such as compliance actuation [3], antagonistic actuation [4, 5], reconfigurable design [6], and more recently the use of stiffness tuneable material [7], and morphing structures [8] are employed. The control of damping to achieve a desired stiffness is shown to be important too, for task accuracy and control stability [9, 10]. However, compliance has disadvantages such as reduced control bandwidth, stability issues, and underdamped modes where high stiffness modes are required to achieve precision in tasks involving working against external loads [10].

Soft continuum manipulators, mostly inspired by octopus arms, snake, land animals' tongue, and trunk, with high inherent dexterity and reconfigurability, have become an attractive candidate for safe manipulation and explorations in surgical and space robotic applications in recent years. The passive shape adaptation and large reachable configuration space features of this class of manipulators due to their highly deformable nature made them a perfect choice for minimally invasive insertion of surgical tools in the confined maze-like space in a robotic surgery [11, 12]. Among the continuum manipulator designs, braided pneumatic and hydraulic actuators provide a uniform homogeneous deformation, robust geometry and force control, and linear and reversible behavior [13–16] compared to the non-braided versions [17–19] which circumferential expansion limits their application in confined space. Besides, accuracy in precise tasks is a challenge with highly flexible structures for which stiffness variable designs based on jamming, smart material, antagonistic actuation, and morphing structures have been introduced in the recent years [20]. The uncertainty in the material deformation due to highly elastic environment, insufficient flexibility, and lack of control feedback are the limitations of continuum manipulators [21]. While most of the research have been focused on the design and modeling of soft

manipulators, methods of stiffness control for soft media have recently shown to be important for efficient minimalist actuation, minimal invasive interaction, and control and sensing precision [22].

Jamming concept and stiffness tunable material are used in variable compliance robotic studies [20]. Jamming concept, for stiffness control through modulating the Coulomb friction and viscous damping between the jammed media, has been utilized in the design of stiffness controllable actuators [23], flexible manipulators [24], variable stiffness joints [25], rehabilitation devices [26], stiffness displays [27], biomimetic organs [28], reconfigurable mechanisms [29], and grippers [30] of which a comprehensive review is presented in [20]. The comparative study by Wall et al. on granular, layer, and scale jamming used in a selective stiffness controllable pneumatic actuator, PneuFlex, showed the layer jamming arrangement to be the most capable design with an eight times increase in the stiffens and 2.23 times increase in the resisting force [23]. Tendon driven jamming was introduced recently to overcome portability limitation of pneumatic enabled jamming in underwater and space applications where a continuum rod flexural stiffness is controlled by modulating the shear friction force between the scales [28, 31] and helical rings [32]. The resulting Coulomb damping opposes the inter-layer shear forces caused by the external load bending momentum.

Thermo-active stiffness tuneable structures and materials have attracted many research in the past few years due to their high range of stiffness change, easy electrical modulation through heating, and possible 3D printing fabrication [33]. Low melting point (LMP) alloy such as field's metal [33–39] and LMP composite material with inherent thermal instability such as wax [40] and ABS which are used as the base material in many standard 3D printing devices have been utilized to design 3D printable thermally stiffness tunable structures [41–44]. As a result, new compound micro actuators capable of actuation and shape fixation with high reversibility and load bearing capacity are designed such as a thermally stiffness tunable actuator fiber in [45] and a thermally tunable shape memory electro-active polymer in [46].

Granular [16] and tendon [47] stiffening methods were investigated for a STIFF-FLOP module recently. Furthermore, we presented a tendon driven scale jamming design inspired by the helical arrangement and morphology of the fish scales (Figures 5.1a and b) to control torsional stiffness of a helical interface cross section for STIFF-FLOP manipulators in our previous work. As a result, we achieved a simpler design and actuation method which, for the first time, provides better wearability, higher stiffening ratio, linear behavior, longer axial stretch, and lower hysteresis [31] compared to the

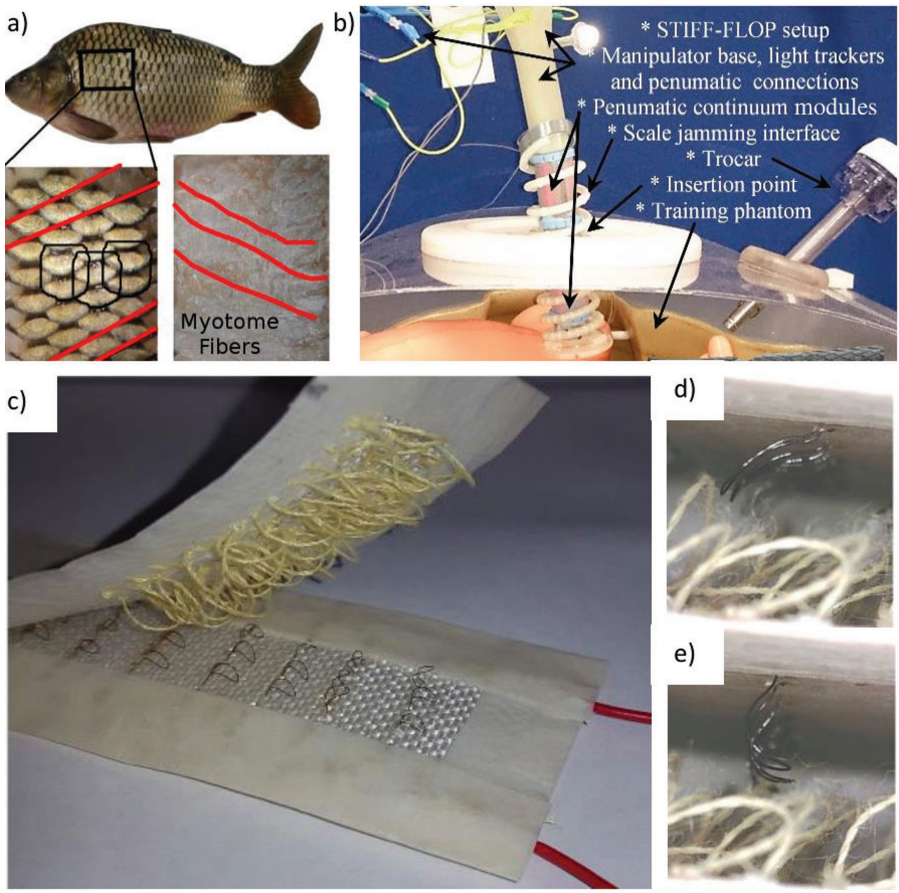

Figure 5.1 Bio-inspired stiffening mechanisms developed for STIFF-FLOP continuum actuators: a scale jamming interface inspired by helical myotome attachment sites and overlapping scales in a Cyprinus carpio fish (a), sample application of the bio-inspired scale jamming interface on a STIFF-FLOP continuum actuator (b) [31], a wearable electro-active Velcro attachment mechanism [48] inspired by stiffening mechanism in natural wood using an interlayer micro hook structure [49] (c), and shape memory alloy hooks' in relaxed (d) and activated (e) states [48].

previous stiffenong solutions for STIFF-FLOP [16, 47] and, to the best of our knowledge, other available locking and jamming designs in literature [20]. However, local and directional stiffness control of continuum manipulators are still challenging. While usually the normal forces on the jammed surfaces are controlled for stiffening, in our recent work, we investigated

the idea of using an active attachment mechanisms between the layers based on a novel electro-active velcro using shape memory alloy wire [48] (Figures 5.1c to d).

As the most similar artificial product to a biological tissue, hydrogels are organic soft materials made of crosslinked polymers capable of absorbing great amount of water without losing their initial structure integrity. These chemical crosslinks provide high mechanical strength and long degradation time and have become widely studied as soft actuators [50], micro robots for drug delivery [51], tissue engineering [52], biosensor [53], self-healing structures [54], etc. Active hydrogels show stiffness controllable properties. Most environmentally responsive hydrogels consist of monomers, an initiator, and an accelerator [53, 55]. The fabrication process usually consists of free radical polymerization of low-molecular-weight monomers in aqueous solution with a crosslinking agent. The use of a crosslinker results in a gel that expands due to the monomer/crosslinker concentrations and the polymerization conditions. UV or thermal treatment can be used for the polymerization process based on the selected solvent. The polymerization technique changes the formed gel properties [56, 57].

In this research, we investigate the fabrication and use of an electro-active stiffness tunable poly(sodium acrylate) (pNaAc) hydrogel as presented in [57] with possible application in stiffness controllable continuum manipulators. We focused on the synthesis, characterization, preparation, and possible applications of pNaAc hydrogel. Different properties of an easy to fabricate hydrogel as in [57] are investigated. A conceptual design for a stiffness controllable STIFF-FLOP module is presented based on a porous hydrogel shell with an anisotropic stiffness ion pattern. The use of active hydrogels for stiffness control of continuum mechanisms is a novel concept which our results in this section provide the preliminary understanding about the gel behavior and a proof for such concept. Our approach in using conventional set of tools to fabricate an active hydrogel shows the feasibility of fabrication of such smart material to be used by researchers with limited to no expertise in experimental chemistry.

Materials and methods of our research are presented in Section 5.2, where fabrication of two slightly different pNaAc hydrogels is discussed. Experiments on the samples' swelling and stiffness properties and a conceptual design for a porous pNaAc hydrogel shell for continuum manipulators are discussed in Section 5.3. Finally, conclusions are presented in Section 5.4

5.2 Materials and Methods

Active hydrogels usually consist of monomers, an initiator, and an accelerator [55]. Ammonium persulfate (APS) is usually used as an initiator and tetramethylethylenediamine (TEMED) as a catalyst. The persulfate can be used to convert monomers to free radicals. The free radicals react with unactivated monomers and begin the polymerization process. The APS (initiator) and TEMED (accelerator) are added to an aqueous solution of albumin [58], polyacrylate [59], polyvynil alcohol [60], or N,N-methylenebis(acrylamide) [57] based on the required hydrogel properties.

Among the different recent fabrication methods introduced in the literature, we used an easy method as in [57], with some changes in the mixture and mole ratios, to fabricate an electro- and thermo-active hydrogel, cable of generating mechanical motion and stiffness variation in dry and wet conditions. Apart from the necessary chemical compounds and some conventional tools for measuring and mixing, this method needs only a conventional low power (70 W) nail polishing UV dryer and a conventional kitchen oven for polymerization and drying processes. Acrylamide (AAm, Sigma: www.sigmaaldrich.com), anhydrous acrylic acid 99% (AA, Sigma), poly(N-isopropylacrylamide) (pNIPAAm, Sigma), N,N-methylenebis(acrylamide) (Sigma), ammonium persulfate (APS, Sigma), NaCl, N,N,NN-tetramethylethylenediamine 99.5% (TEMED, Sigma), agarose LE (Sigma), sodium hydroxide (Fisher Scientific: www.fishersci.co.uk), ethylenediaminetetraacetic acid (EDTA, Sigma), and Milli-Q deionized water (18.2 MΩ cm, Amazon) are used for the fabrication of the hydrogel straps as in [57]. Copper anode wires (Cu^{2+}, 1 mm diameter, Alfa Aesar: www.alfa.com), ethanol, and deionized distilled water (Amazon) are used for providing aquatic or dry test environment, electric activation, and material recovery.

5.2.1 Active Hydrogel Preparation

Following the procedure in [57], we fabricated two poly(sodium acrylate) (pNaAc) hydrogel samples with slightly different compound ratios considering our stiffness controllable application. The first strap sample, to be formed in a helical shape after ion pattern printing (Figure 5.2), is prepared by free radical polymerization in an aqueous solution, combining 3 mole (M) concentration of poly(N-isopropylacrylamide) (pNIPAAm) monomer, as a stimuli responsive substance, and N,N-methylenebis(acrylamide) as the crosslinker with mole ratio (divinyl to vinyl monomers) of 1:100. It was

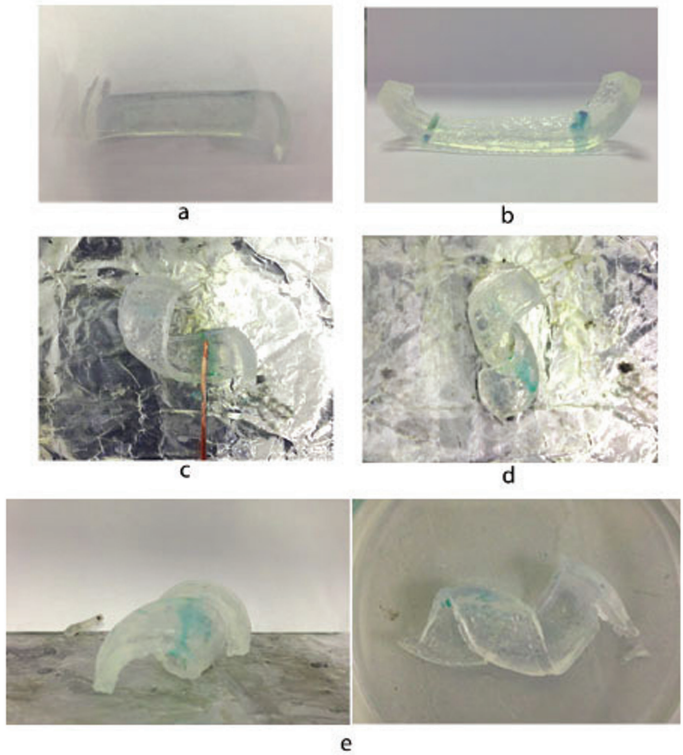

Figure 5.2 A sample electro-active swelling hydrogel strap with 1 mm thickness (a), printed ionic patterns with light blue color on the two sides of the strap (b), printing ionic patterns with a copper wire (Cu^{2+}) (c), helix formation of the strap due to mechanical shrinkage at the printed ionic pattern (d), and side and top views of the final helical hydrogel sample when it is still wet (e).

mixed with fluorescein isothiocyanate (FITC 5 m diameter) for electrostatic stabilization. As a result, a gel with a large swelling and stiffness variation response in different aquatic solutions is fabricated. It was prepared with Milli-Q deionized water (18.2 MΩ cm) and ethanol solution with 4:1 ratio. The solution was subjected to 70 W UV light for 1 hour and then dried at 60°C temperature in an oven for free radical polymerization process.

The second strap sample, to be formed in a cylindrical shape after ion pattern printing (Figure 5.3), is prepared by free radical polymerization of AAm monomer with a small amount of N,N-methylenebis(acrylamide) as

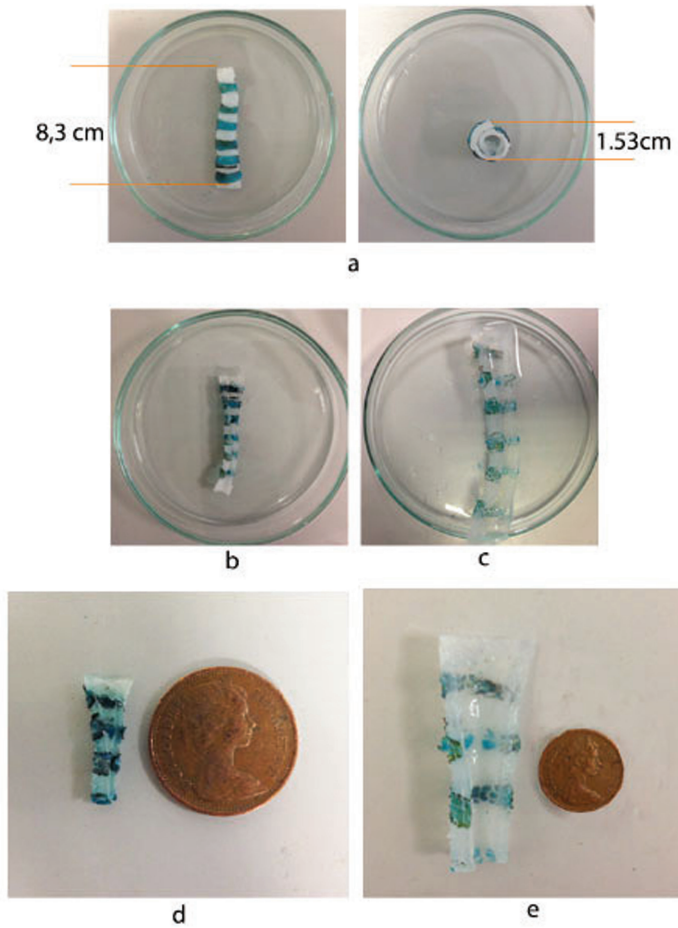

Figure 5.3 A sample electro-active swelling hydrogel with close parallel ionic printed patterns, forming a cylindrical shape, in top and side views (a), the sample after swelling due to immersing in 1:4 ethanol aquatic solution for 3 minutes (b) and in dry state after immersing in ethanol (c), the sample size in comparison to a British one pence coin in dry (d) and wet (e) conditions. The sample retains its cylindrical shape in dry and wet conditions regardless of 180% change in its size due to swelling and a softer structure in the swelled condition.

the crosslinker. Five grams of AA-AAm mixture is mixed with equimolar amounts of sodium hydroxide, based on the number of AA moles (mixture I); 240 mg of N,N-methylenebis(acrylamide) was added to 40 mg of APS which then was dissolved in distilled water and added to the mixture I (mixture II); 0.024 mL of TEMED was added to the mixture II and the product is molded

in a thin layer shape. The equilibrium swelling ratio is achieved based on the crosslinker mole ratio (divinyl to vinyl monomers) which was set to be 5:100% here. Leaving the mixture for a whole day in the room ambient, the polymerization process produces a dry hydrogel that can be cut in the desired shape. The dry pNaAc hydrogel was immersed in four aquatic solutions, 1) distilled water and ethanol (EtOH), 2) distilled water, 3) deionized water, and 4) tap water for over 2 hours, to find the best swelling ratio, and then dried in 70°C using the oven. Watering and drying steps are repeated if the final mechanical properties are not satisfactory.

5.2.2 Active Hydrogel Properties and Ion Pattern Printing

The pNaAc hydrogels swell when are placed in an aquatic solution, usually for more than 3 minutes. The watering can be reversed, and the sample shrinks and hardens by putting it in ethanol for about 2 hours. The swelling deformation can be used as a mechanical actuation method. Besides, different electro-mechanical responses, e.g., swallowing, bending, and twisting can be achieved by ion printing, creating an anisotropic stiffness network consisting of conductive particles. This is done by applying 9-V DC through a copper wire (Cu^{2+}, anode) while placing the hydrogel straps on an aluminum foil (cathode). As a result, two adjacent sodium ions in the gel move toward a cupric ion and bind to the gel carboxylic groups. This leaves a ionized pattern with light blue color that shrinks and stiffens compared to the rest of the gel. The sample shape is fixed, showing a shape memory feature in Figures 5.2a to c. Figure 5.2 shows a sample with two ionic patterns at each end that bring the hydrogel strap to a helical shape and Figure 5.3a shows a sample with closer parallel patterns that forms a cylindrical shape. The samples maintain their shape while absorbing water solution as in Figures 5.2e and 5.3b,c. The inhomogeneous stiffness due to the ionic patterns causes an even more local shrinkage of the sample when immersed and dried in ethanol. The electric field deforms the hydrogel in air. This deformation is reversible by applying a reversed field. Both the local shrinkage due to the ionic actuation and watering-ethanol drying cycles of a ion-printed gel can be used as actuation mechanisms for a hydrogel actuator [57]. We investigated the watering-ethanol drying cycle here as a stiffening mechanism where ion patterns help bringing the structure to more stable and stiffer, e.g., helical or cylindrical, configurations. After multiple watering-ethanol drying cycles, we used the resulted dried contracted hydrogel in our stiffness tests.

5.3 Experiments and Discussion

5.3.1 Swelling Test

The dried hydrogels in ethanol swell up to 100% for the helical (Figure 5.2e) and 180% for the cylindrical (Figures 5.3b and c) shape strap after are immersed in deionized water for about 3 minutes (Figure 5.4) while maintaining but loosing the grip of its programmed shape. The sample can be dried in ethanol and immersed again with no noticable hysteresis buildup in our six trials. Leaving the swelled samples in the room temperature to dry disintegrates the hydrogel and breaks their structure as the water evaporates, while the dried sample in ethanol can be left for a long time unchanged in the room temperature, 1 week in our case, with no noticeable change in its swelling ability, final volume, and stiffness. The hardened gel in ethanol turns from a white transparent to a yellow cloudy color after being left in the room temperature for a while (Figure 5.5a). Despite the low stiffness of the swelled hydrogel in water, the dried samples in ethanol shrink and hold a stiff, hard to break, or deform shape, with a harder grip to the programmed shape. To achieve higher swelling ratios (lower stiffness), the sample needs to be fully dried first. Different aqueous solutions were tested, showing the best swelling results for deionized and common tap (with unknown chemical impurity) water while ethanol solution results in the least swelling ratio.

5.3.2 Stiffness Test

A helical pNaAc hydrogel strap, with size 55 $\times$ 10 $\times$ 1 mm when swells, is prepared for stiffness test after initiating in 70 W UV light for 30 minutes,

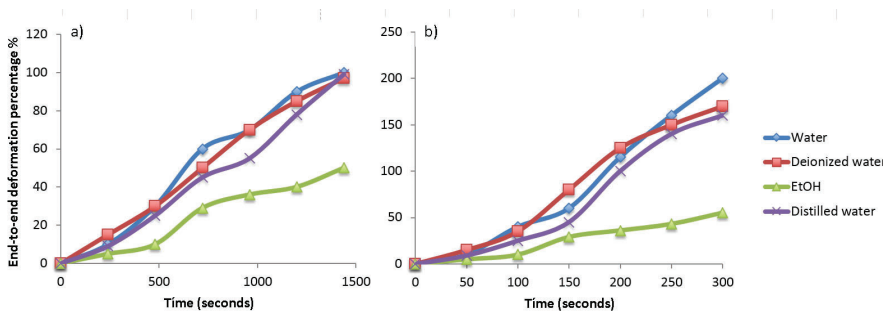

Figure 5.4 End-to-end deformation percentage (%) after swelling in different aquatic solutions for the pNaAc helical (Figure 5.2) (a) and cylindrical (Figure 5.3) (b) hydrogel samples.

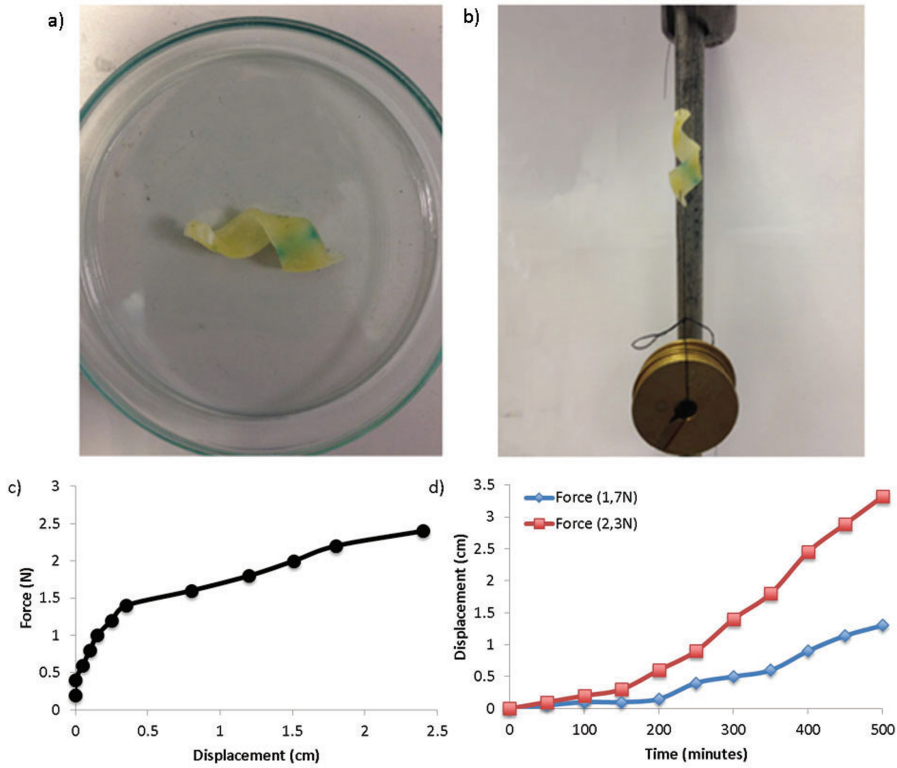

Figure 5.5 Hardened and dried electro-active hydrogel of Figure 5.2 in ethanol and room temperature (a), tension tests (b), force–displacement (c), and displacement–time (d) graphs for the simple tension experiments.

equilibrated in dionized water for 30 minutes, hardened in ethanol, and left in room temperature to completely dry for 3 days. The force–displacement and displacement–time graphs for the simple tension experiments are presented in Figures 5.5c and d, showing an initial quasi-static elastic deformation region with yield force of 1.5 N and stiffness of 4.2 KN/m followed by an accelerating linear plastic deformation region with resisting force up to 2.5 N and stiffness of 0.5 KN/m (Figure 5.5c). The structure breaks at 2.8 N. The hydrogel elasticity remains almost constant for 150 seconds. However, it decreases rapidly over time under a constant force (Figure 5.5d) which can be due to propagation of cracks in the gel structure. The hydrogel stiffness is negligibly low after placing it in an aquatic solution for 3 minutes. The large stiffness variation achieved by changing the ethanol saturation in an aquatic

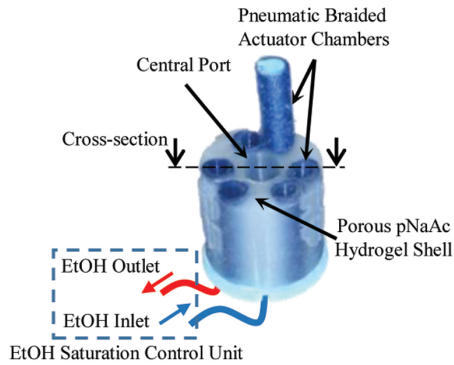

Figure 5.6 Conceptual design for a STIFF-FLOP module with a cylindrical porous pNaAc hydrogel with ion-printed ring patterns. The hydrogel stiffness is controlled by changing the ethanol saturation in EtOH solution, that fills the hydrogel shell pores, using a set of micro pumps and a solution saturation control unit.

solution can be exploited for stiffness variable applications such as stiffness controllable continuum robots and stiffness displays. A conceptual design is presented in Figure 5.6 where the body shell of a STIFF-FLOP manipulator is filled with a porous pNaAc hydrogel while the pores are filled with an aquatic ethanol solution. Changing the ethanol saturation by pumping in new solution with different ethanol saturation in the gel pores while draining out the previous solution results in a change in the structure stiffness. The slow stiffness variation is not a problem in medical tasks with mostly quasi-static motions. Printing ionic patterns, i.e. parallel rings on the structure, strengthen the structure by programming a cylindrical shape memory that can act as an external reinforcement for achieving even higher stiffness values.

5.4 Conclusion and Future Works

Electroactive hydrogels are usually formed based on monomers, an initiator, and an accelerator. Following the procedure presented in [57], we fabricated an electro- and thermo-active pNaAc hydrogel on which ionic patterns with anisotropic stiffness are printed using a copper wire as the anode and an aluminum sheet as the cathode. The ionic patterns shrink and stiffen bringing the gel to a programmed complex geometrical shape, helix and cylindrical in our case. The ionization process is reversible by reversing the electric field which can be used to design an electro-active hydrogel actuator. The hydrogel softens and swells up to two times of its original size in an aquatic

solution while preserving its programmed shape. The observed stiffness variation (0–4.2 KN/m) by changing the ethanol saturation in an aquatic ethanol solution can be exploited to design stiffness controllable continuum manipulators or stiffness displays. A conceptual design for a stiffness controllable STIFF-FLOP module is presented with porous pNaAc hydrogel shell and ring-shaped ionic patterns, the pores of which are filled with aquatic ethanol solution. The structure stiffness can be controlled by changing the ethanol solution ratio using micropumps and a control unit to monitor and modulate the solution ratio. We plan to fabricate the proposed design in a future research.

References

[1] Albu-Schäffer, A., and Bicchi, A. (2016). "Actuators for Soft Robotics," in *Springer Handbook of Robotics*, eds B. Siciliano and O. Khatib (Cham: Springer International Publishing), 499–530.

[2] Tomori, H., Nagai, S., Majima, T., and Nakamura, T. (2013). "Variable impedance control with an artificial muscle manipulator using instantaneous force and MR brake," in *Proceeding of 2013 IEEE/RSJ International Conference on Intelligent Robots and Systems*, Tokyo, 5396–5403.

[3] Zhu, Y., Yang, J., Jin, H., Zang, X., and Zhao, J. (2014). "Design and evaluation of a parallel-series elastic actuator for lower limb exoskeletons," in *Proceeding of 2014 IEEE International Conference on Robotics and Automation (ICRA)*, Hong Kong, 1335–1340.

[4] Maghooa, F., Stilli, A., Noh, Y., Althoefer, K., and Wurdemann, H. A. (2015). "Tendon and pressure actuation for a bio-inspired manipulator based on an antagonistic principle," in *Proceedings of 2015 IEEE International Conference on Robotics and Automation (ICRA)*, Seattle, WA, 2556–2561.

[5] Chalon, M., Friedl, W., Reinecke, J.,Wimboeck, T., and Albu-Schaeffer, A. (2011). "Impedance control of a non-linearly coupled tendon driven thumb," in *Proceeding of 2011 IEEE/RSJ International Conference on Intelligent Robots and Systems*, San Francisco, CA, 4215–4221.

[6] Müller, U. K., and Van Leeuwen, J. L. (2006). Undulatory fish swimming: from muscles to flow. *Fish Fish*. 7, 84–103.

[7] Yuse, K., Guyomar, D., Audigier, D., Eddiai, A., Meddad, M., and Boughaleb, Y. (2013). Adaptive control of stiffness by electroactive polyurethane. *Sens. Actuators A Phys.* 189, 80–85.

[8] Luo, Q., and Tong, L. (2013). Adaptive pressure-controlled cellular structures for shape morphing I: design and analysis. *Smart Mater. Struct*. 22, 055014.

[9] Laffranchi, M., Tsagarakis, N. G., and Caldwell, D. G. (2013). Compact arm: a compliant manipulator with intrinsic variable physical damping. *Robotics* 8, 225–232.

[10] Erden, M. S., and Billard, A. (2015). Hand impedance measurements during interactive manual welding with a robot. *IEEE Trans. Robot*. 31, 168–179.

[11] Burgner-Kahrs, J., Rucker, D. C., and Choset, H. (2015). "Continuum robots for medical applications: a survey. *IEEE Trans. Robot*. 31, 1261–1280.

[12] Cianchetti, M., and Menciassi, A. (2017). "Soft Robots in Surgery," in *Soft Robotics: Trends, Applications and Challenges*: *Biosystems and Biorobotics*, Vol. 9, 1st Edn, eds C. Laschi, J. Rossiter, F. Iida, M. Cianchetti and L. Margheri (Cham: Springer International Publishing), 75–85.

[13] Suzumori, K., Iikura, S., and Tanaka, H. (1991). "Flexible microactuator for miniature robots," in *Proceedings of the IEEE Micro Electro Mechanical Systems*, Nara, 204–209.

[14] McMahan, W., Chitrakaran, V., Csencsits, M., Dawson, D., Walker, I. D., Jones, B., et al. (2006). "Field trials and testing of the OcotArm continuum manipulator," in *Proceedings of the 2006 IEEE International Conference on Robotics and Automation (ICRA)*, 2336–2341.

[15] Fraś, J., Czarnowski, J., Maciaś, M., Główka, J., Cianchetti, M., and Menciassi, A. (2015). "New STIFF-FLOP module construction idea for improved actuation and sensing," in *Proceedings of 2015 IEEE International Conference on Robotics and Automation (ICRA)*, Seattle, WA, 2901–2906.

[16] Cianchetti, M., Ranzani, T., Gerboni, G., De Falco, I., Laschi, C., and Menciassi, A. (2013). "STIFF-FLOP surgical manipulator: mechanical design and experimental characterization of the single module," in *Proceedings of the IEEE International Conference on Intelligent Robots and Systems (IROS)*, Tokyo, 3576–3581.

[17] Ranzani, T., Cianchetti, M., Gerboni, G., Falco, I. D., Petroni, G., and Menciassi, A. (2013). "A modular soft manipulator with variable stiffness," in *Proceedings of the 3rd Joint Workshop on New Technologies for Computer/Robot Assisted Surgery*, Verona.

[18] Suzumori, K., Maeda, T., Watanabe, H., and Hisada, T. (1997). "Fiberless flexible microactuator designed by finite-element method. *IEEE/ASME Trans. Mechatron*. 2, 281–286.

[19] Marchese, A. D., and Rus, D. (2016). Design, kinematics, and control of a soft spatial fluidic elastomer manipulator. *Int. J. Robot. Res*. 35, 840–869.

[20] Blanc, L., Delchambre, A., and Lambert, P. (2017). Flexible medical devices: review of controllable stiffness solutions. *Actuators* 6:23.

[21] Sareh, S., Jiang, A., Faragasso, A., Noh, Y., Nanayakkara, T., Dasgupta, P., et al. (2014). "Bio-inspired tactile sensor sleeve for surgical soft manipulators," in *Proceeding of 2014 IEEE International Conference on Robotics and Automation (ICRA)*, Hong Kong, 1454–1459.

[22] Manti, M., Cacucciolo, V., and Cianchetti, M. (2016). Stiffening in soft robotics: a review of the state of the art. *IEEE Robot. Automat. Magaz.* 23, 93–106.

[23] Wall, V., Deimel, R., and Brock, O. (2015). "Selective stiffening of soft actuators based on jamming," in *Proceeding of 2015 IEEE International Conference on Robotics and Automation (ICRA)*, Seattle, WA, 252–257.

[24] Cheng, N. G., Lobovsky, M. B., Keating, S. J., Setapen, A. M., Gero, K. I., Hosoi, A. E., et al. (2012). "Design and analysis of a robust, low-cost, highly articulated manipulator enabled by jamming of granular media," in *Proceedings—IEEE International Conference on Robotics and Automation*, Saint Paul, MN. 4328–4333.

[25] Jiang, A., Ataollahi, A., Althoefer, K., Dasgupta, P., and Nanayakkara, T. (2012). "A variable stiffness joint by granular jamming," in *Proceedings of the ASME Design Engineering Technical Conference, Parts A and B*, Vol. 4, Chicago, IL, 267–275.

[26] Hauser, S., Eckert, P., Tuleu, A., and Ijspeert, A. (2016). "Friction and damping of a compliant foot based on granular jamming for legged robots," in *Proceedings of the 2016 6th IEEE International Conference on Biomedical Robotics and Biomechatronics (BioRob)*, Singapore, 1160–1165.

[27] Stanley, A. A., and Okamura, A. M. (2016). "Deformable model-based methods for shape control of a haptic jamming surface. *Visual. Comput. Graph. IEEE Trans.* 23, 1029–1041.

[28] Santiago, J. L. C., Godage, I. S., Gonthina, P., and Walker, I. D. (2016). "Soft robots and kangaroo tails: modulating compliance in continuum structures through mechanical layer jamming. *Soft Robot*. 3, 54–63.

[29] Jiang, A., Aste, T., Dasgupta, P., Althoefer, K., and Nanayakkara, T. (2013). Granular jamming transitions for a robotic mechanism. *AIP Confer. Proc*. 1542, 385–388.

[30] Cheng, N., Amend, J., Farrell, T., Latour, D., Martinez, C., Johansson, J., A. et al. (2016). Prosthetic jamming terminal device: a case study of untethered soft robotics. *Soft Robot*. 3, 205–212.

[31] Sadati, S., Noh, Y., Naghibi, S. E., Kaspar, A., and Nanayakkara, T. (2015). "Stiffness control of soft robotic manipulator for minimally invasive surgery (MIS) using scale jamming," in *Proceedings of the International Conference on Intelligent Robotics and Applications (ICIRA)*, *Lecture Notes in Computer Science*, (Portsmouth: Springer International Publishing), 141–151.

[32] Ataollahi, A., Karim, R., Fallah, A. S., Rhode, K., Razavi, R., L. Seneviratne, D., et al. (2016). Three-degree-of-freedom MR-compatible multisegment cardiac catheter steering mechanism. *IEEE Trans. Biomed. Eng.* 63, 2425–2435.

[33] Van Meerbeek, I. M., Mac Murray, B. C., Kim, J. W., Robinson, S. S., Zou, P. X., Silberstein, M. N., et al. (2016). Morphing metal and elastomer bicontinuous foams for reversible stiffness, shape memory, and self-healing soft machines. *Adv. Mater.* 28, 2801–2806.

[34] Shintake, J., Schubert, B., Rosset, S., Shea, H., and Floreano, D. (2015). "Variable Stiffness Actuator for Soft Robotics Using Dielectric Elastomer and Low-Melting-Point Alloy Soft state," in *Proceedings of the IEEE/RSJ International Conference on Intelligent Robots and Systems (IROS)*, Hamburg, 1097–1102.

[35] Tonazzini, A., Mintchev, S., Schubert, B., Mazzolai, B., Shintake, J., and Floreano, D. (2016). Variable stiffness fiber with self-healing capability. *Adv. Mater*. 28, 10142–10148.

[36] Jeong, S. H. (2016). *Liquids Matter in Compliant Microsystems*. Uppsala: Uppsala University.

[37] Janbaz, S., Hedayati, R., and Zadpoor, A. A. (2016). Programming the shape-shifting of flat soft matter: from self-rolling/self-twisting materials to self-folding origami. *Mater. Horiz.* 3, 536–547.

[38] Alambeigi, F., Seifabadi, R., and Armand, M. (2016). "A continuum manipulator with phase changing alloy," in *Proceedings of the IEEE International Conference on Robotics and Automation*, Stockholm, 758–764.

[39] Wang, W., Rodrigue, H., and Ahn, S.-H. (2016). "Deployable soft composite structures. *Sci. Rep.* 6, 20869–20869.

[40] Cheng, N. G., Gopinath, A., Wang, L., Iagnemma, K., and Hosoi, A. E., (2014). Thermally tunable, self-healing composites for soft robotic applications. *Macromol. Mater. Eng.* 299, 1279–1284.

[41] Yang, Y., and Chen, Y. (2016). "Novel design and 3d printing of variable stiffness robotic fingers based on shape memory polymer," in *Proceedings of the 2016 6th IEEE International Conference on Biomedical Robotics and Biomechatronics (BioRob)*, Singapore, 195–200.

[42] Yang, Y., Chen, Y., Li, Y., and Chen, M. Z. (2016). "3d printing of variable stiffness hyper – redundant robotic arm," in *Proceedings of the 2016 IEEE International Conference on Robotics and Automation (ICRA)*, Stockholm, 3871–3877.

[43] Lipton, J. I., and Lipson, H. (2016). 3d printing variable stiffness foams using viscous thread instability. *Sci. Rep.* 6:29996.

[44] Yang, Y., Chen, Y. H., Wei, Y., and Li, Y. (2016). Novel design and 3d printing of variable stiffness robotic grippers. *J. Mech. Robot.* 8, 134–143.

[45] Yuen, M. C., Bilodeau, R. A., and Kramer, R. K. (2016). Active variable stiffness fabric. *IEEE Robot. Autom. Lett.* 1, 708–715.

[46] Yao, Y., Zhou, T., Wang, J., Li, Z., Lu, H., Liu, Y., et al. (2016). 'Two way' shape memory composites based on electroactive polymer and thermoplastic membrane. *Comp. A Appl. Sci. Manuf.* 90, 502–509.

[47] Shiva, A., Stilli, A., Noh, Y., Faragasso, A., Falco, I. D., Gerboni, G., et al. (2016). Tendon-based stiffening for a pneumatically actuated soft manipulator. *IEEE Robot. Autom. Lett.* 1, 632–637.

[48] Afrisal, H., Sadati, S., and Nanayakkara, T. (2016). A bio-inspired electro-active velcro mechanism using shape memory alloy for wearable and stiffness controllable layers," in *Proceedings of the 2016 9th International Conference on Information and Automation for Sustainability (ICIAfS)* (Rome: IEEE), 1–6.

[49] Kretschmann, D. (2003). Nature materials: velcro mechanics in wood. *Nat. Mater.* 2, 775–776.

[50] Xu, X., Zhang, Q., Yu, Y., Chen, W., Hu, H., and Li, H. (2016). Naturally dried graphene aerogels with superelasticity and tunable poisson's ratio. *Adv. Mater.* 28, 9223–9230.

[51] Kwon, G. H., Park, J. Y., Kim, J. Y., Frisk, M. L., Beebe, D. J., and Lee, S. H. (2008). Biomimetic soft multifunctional miniature aquabots. *Small* 4, 2148–2153.

[52] Ebara, M., Kotsuchibashi, Y., Narain, R., Idota, N., Kim, Y.-J., Hoffman, J. M., et al. (2014). *Smart Biomaterials*. Berlin: Springer.

[53] Jones, C. D., and Steed, J. W. (2016). Gels with sense: supramolecular materials that respond to heat, light and sound. *Chem. Soc. Rev.* 45:c6cs00435k.

[54] Taylor, D. L., and In Het Panhuis, M. (2016). Self-healing hydrogels. *Adv. Mater*. 28, 9060–9093.

[55] Kuckling, D. (2009). Responsive hydrogel layers—From synthesis to applications. *Coll. Polym. Sci.* 287, 881–891.

[56] Osada, Y., and Gong, J.-P. (1998). Soft and wet materials: polymer gels. *Adv. Mater.* 10, 827–837.

[57] Palleau, E., Morales, D., Dickey, M. D., and Velev, O. D. (2013). Reversible patterning and actuation of hydrogels by electrically assisted ionoprinting. *Nat. Commun*. 4:2257.

[58] Park, K. (1988). Enzyme-digestible swelling hydrogels as platforms for long-term oral drug delivery: synthesis and characterization. *Biomaterials* 9, 435–441.

[59] Giammona, G., Pitarresi, G., Cavallaro, G., Buscemi, S., and Saiano, F. (1999). New biodegradable hydrogels based on a photocrosslinkable modified polyaspartamide: synthesis and characterization. *Biochim. Biophys. Acta* 1428, 29–38.

[60] Martens, P., and Anseth, K. S. (2000). Characterization of hydrogels formed from acrylate modified poly(vinyl alcohol) macromers. *Polymer* 41, 7715–7722.